FRENCH-UKRAINIAN JOURNAL OF CHEMISTRY (**2022**, VOLUME **10**, ISSUE **01**)

Complexation of 1,3-dihetaryl-5-phenyl-2-pyrazoline Derivatives with Polyvalent Metal Ions: Quantum Chemical Modeling and Experimental Investigation

Andrii Chumak, Ruslana Khodzhaeva, Olena Kharchenko, Volodymyr Kotliar,
Oleksii Kolomoitsev, Andrey Doroshenko*

V. N. Karazin Kharkiv National University, Svobody Sq., 4, Kharkiv 61022, Ukraine

andrey.o.doroshenko@gmail.com

Keywords: *1,3,5-triaryl-2-pyrazoline, pyridine, benzimidazole, benzothiazole, spectrophotometric and fluorescence analysis, complexation, polyvalent metal ions, quantum-chemical calculations, Bader's atoms-in-molecules (AIM) theory.*

1,3,5-Triaryl-2-pyrazoline derivatives with a pyridine ring in position 1 and 2-benzimidazolyl or 2-benzothiazolyl bicycles in position 3 were synthesized. Spectral properties in solvents of similar polarity, i.e. aprotic acetonitrile and in protic methanol, were studied, complexation with cadmium and mercury ions in acetonitrile was elucidated as well. Quantum-chemical modeling with application of the elements of Bader's atoms-in-molecules (AIM) theory of the title molecules conformational structure and 1:1 stoichiometry complexes formed with polyvalent metals of various nature (Mg, Zn, Cd, Pb, Hg, Ba) was conducted. The principal possibility of “nitrogen-sulfur” switching of the metal ions binding sites for the benzothiazole derivative was revealed, and makes possible to classify this compound as “smart ligand”.

Introduction

Molecular design and investigation of aromatic organic compounds as analytical reagents for polyvalent metal ions remain highly important for several decades [1-6]. These studies have been triggered by the development of manufacturing of modern equipment for spectrophotometric and fluorometric analysis, which allows them to be more sensitive, cheap and convenient to fit up stationary and mobile laboratories for industrial, environmental, medical control etc. 1,3,5-Triaryl-2-pyrazoline derivatives with a pyridine ring in position 1 and 2-benzimidazolyl or 2-benzothiazolyl bicycles in position 3 were synthesized. Their spectral properties in solvents of similar polarity, i.e. aprotic acetonitrile and in protic methanol, were studied. Their complexation efficiency with cadmium and mercury ions in acetonitrile was determined using spectrophotometric and spectrofluorimetric methods. Quantum-chemical modeling of their conformational structure and complexes formed with polyvalent metals of various nature (Mg, Zn, Cd, Pb, Hg, Ba) in a stoichiometric ratio of 1:1 was conducted. Obtained results are analyzed using the elements of Bader's atoms-in-molecules (AIM) theory. The interaction with double-charged metal ions has been revealed to occur with the participation of three binding sites in the studied organic ligands: the nitrogen atom of pyridine ring in position 1, the nitrogen atom of the pyrazoline ring in position 2, and the nitrogen or sulfur atom of the heterocycle in position 3. Thus, in all cases, tridentate chelate cavity is formed where the pyrazoline ring and the heterocycle in position 3 demonstrate the strongest binding with cations. In the conformation where cation’s coordination with the benzothiazole sulfur atom is possible, stronger coordination bonds are formed with pyrazoline and pyridine rings nitrogen atoms. The principal possibility of “nitrogen-sulfur” switching of the metal ions binding sites for the benzothiazole derivative was revealed. This fact makes it possible to classify the investigated pyrazoline derivatives as “smart ligands”.

Traditionally, search for metal ions indicators includes derivatives of spiropyrane [7, 8], pyridine [9-12], fluorescein [13, 14], rhodamine [15-22] and flavonol [23-29] etc.

Heteroaromatic compounds with closely disposed nucleophilic centers with potential to polyvalent metal ions binding can be considered as "smart ligands", which are able to adjust the three-dimensional structure of their binding sites to the size and physicochemical characteristics of individual ions. The definition "smart ligands" was commonly used in biophysics [30, 31], referring to the selective interaction of low molecular weight organic compounds with biological macromolecules, but in our opinion, its use in the field of analytical detection of metals [32] is possible as well.

Our recent work [33] presented the synthesis of a series of 1,3,5-triarylpyrazoline derivatives with o-hydroxy group in the benzene cycle in position 3 and pyridine or 8-hydroxyquinoline moiety in position 1 of the pyrazoline cycle. Other subjects of that work included spectral properties, intramolecular proton phototransfer reaction and qualitative study of complexation with polyvalent metal ions. It was also suggested that the binding centers for metal ions of different nature could be switched.

The subject matter covered in this work, which is the continuation of the previous topic, is polyheterocyclic pyrazoline derivatives with benzimidazole or benzothiazole bicycle in position 3 and pyridine cycle in position 1. Quantum chemical calculations have been applied to model metal ions binding and to determine complexation center nature.

Experimental part

^{1}H NMR spectra were registered with a Varian MR-400 spectrometer. Electronic absorption spectra were measured with the

Hitachi U-3210 spectrophotometer; fluorescence spectra and quantum yields – with the *Hitachi 850* fluorimeter at a test substance concentration of 10^{-4}-10^{-5} mol/l, an absorbing layer thickness of 10 mm and an excitation wavelength of 360 nm.

Quinine bisulfate in 0.5 M aqueous H_2SO_4 ($\varphi = 0.546$) [34] was used as a reference to determine fluorescence quantum yields.

Experimental studies of the complexation of compounds **3a,b** with cadmium and mercury ions in acetonitrile was conducted with the help of spectrophotometric and fluorimetric methods using their salts - $Cd(NO_3)_2$ and $Hg(OCOCH_3)_2$.

Quantum-chemical calculations were performed with electron density functional theory (DFT) method by means of the Gaussian 09 [35] software package using the electron density functional M06-2x [36] and an orbital basis cc-PVDZ [37] for light atoms and ADZP [38, 39] (which takes into account internal electronic levels as well) - for heavy atoms. The analysis of electron density redistribution in the studied molecules and their complexes with metal ions was carried out using the elements of the Bader' AIM theory [40-42] with the help of the AIM2000 [43] software. The computational time involving the extended ADZP basis for heavy atoms increases significantly in comparison with pseudopotential LanL2DZ [44], which we tested in our preliminary studies. However, wave functions of the complexes obtained in the latter case could not be processed using any kind of the software packages that implement AIM-analysis.

The investigated derivatives of 1,3,5-triaryl-2-pyrazoline were synthesized according to the following scheme:

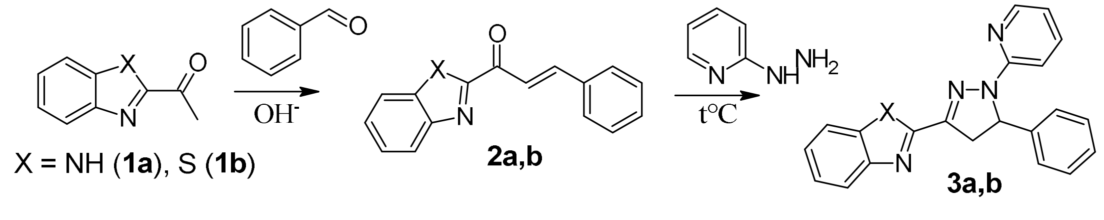

Scheme 1. Synthesis of 1,3,5-triaryl-2-pyrazoline derivatives.

Intermediate chalcone derivatives **2a,b** were obtained via the interaction of heterocyclic acetyl derivatives **1a,b** with an equimolar amount of benzaldehyde under alkaline catalysis in methanol at 50°C. After dissolving initial compounds in alcohol and adding saturated KOH solution, the reaction mixture was kept overnight at the indicated temperature. Than the solvent was removed under reduced pressure, the obtained precipitate was recrystallized from acetonitrile.

The synthesis of target pyrazoline derivatives was carried out by the treatment of stoichiometric amount of corresponding chalcones with 2-pyridylhydrazine in ethanol in the presence of catalytic amount of alkali. After boiling the reaction mixture for 12 hours and removing the solvent under reduced pressure, yellowish crystals were obtained. The products **3a,b** formation was indicated by appearance of green fluorescence, and finally confirmed by the presence of pyrazoline cycle characteristic signals (ABC spin system) in their ^{1}H NMR spectra.

2-[5-phenyl-1-(pyrid-2-yl)-4,5-dihydro-1H-pyrazol-3-yl]-1H- benzimidazole, compound **3a**, ^{1}H NMR (400 MHz, DMSO-d$_6$), δ (ppm): 3.17 (dd, J = 17.9, 5.2 Hz, 1H), 3.99 (dd, J = 17.9, 12.4 Hz, 1H), 5.79 (dd, J = 12.3, 5.0 Hz, 1H), 6.71 (t, 1H), 7.17 (m, 5H), 7.25 (m, 2H), 7.48 (d, 2H), 7.55 (dd, 2H), 7.63 (t, 1H), 7.97 (d, 1H).

2-[5-phenyl-1-(pyrid-2-yl)-4,5-dihydro-1H-pyrazol-3-yl]-benzothiazole, compound **3b**, ^{1}H NMR (400 MHz, DMSO-d$_6$), δ (ppm): 3.21 (dd, J = 17.9, 5.2 Hz, 1H), 4.06 (dd, J = 17.9, 12.4 Hz, 1H), 5.90 (dd, J = 12.3, 5.0 Hz, 1H), 6.78 (t, 1H), 7.20 (m, 3H), 7.27 (m, 2H), 7.45 (m, 3H), 7.67 (t, 1H), 7.97 (m, 3H), 8.09 (d, 1H).

Results and discussions

Experimental study of compounds **3a,b** physicochemical characteristics was preceded by their quantum-chemical modeling. For the formation of complexes with metal ions, the predominant molecular conformation of the organic ligand is critically important, because it determines the geometry of the chelate cavity, the binding site for polyvalent cations. Molecular conformations of the title compounds are presented in **Figure 1**. Additional indices will be used in the corresponding abbreviations to indicate them and adjust spatial proximity of the nitrogen atom of pyrazoline cycle and one of the heteroatoms (N, NH or S) of the benzazole cycle in position 3.

In the molecule of benzimidazole derivative **3a** (**Figure 1**), intramolecular hydrogen bond is not formed, because of *bond path* and the critical point of (3, -1) type was not detected [42]. However, the **3a**$_{\text{NH-N}}$ type conformation is almost 8.7 kcal/mole more energetically favorable, than **3a**$_{\text{N-N}}$. The calculated difference in energies is quite large, because it causes an almost complete shift of a probable conformational equilibrium in favor of the conformer **3a**$_{\text{NH-N}}$. Thus, the complexes formation with metal ions in the case of compound **3a** will require a change in conformation, as the N-H group will interfere with cationic analytes binding to potential complexing sites – unshared electron pairs of nitrogen atoms in imidazole, pyrazoline and pyridine cycles. Besides, in the proton donor medium, the mutual transformation of **3a**$_{\text{NH-N}}$ into **3a**$_{\text{N-N}}$ and back will be significantly facilitated by proton exchange with the environment: the addition of a proton to the N3' atom will result in dissociation of the N1'-H bond. This is equivalent to the rotation of the benzimidazole moiety around the single bond, which connects it with the pyrazoline cycle.

The benzothiazole derivative exists mainly in the **3b**$_{S\text{-}N}$ conformation, which is 5.7 kcal/mole more energetically favorable (the fraction of alternative **3b**$_{N\text{-}N}$ conformation will not exceed 0.1% under equilibrium conditions, as estimated according to Arrhenius). Thus, it is possible to assume a certain probability of participation of the sulfur atom of compound **3b** in the formation of chelate complexes with heavy metal ions.

In both cases, the nitrogen atom of the pyridine ring is spatially close to the nitrogen atom in position 2 of the pyrazoline cycle, forming a potential chelate cavity for cations coordination.

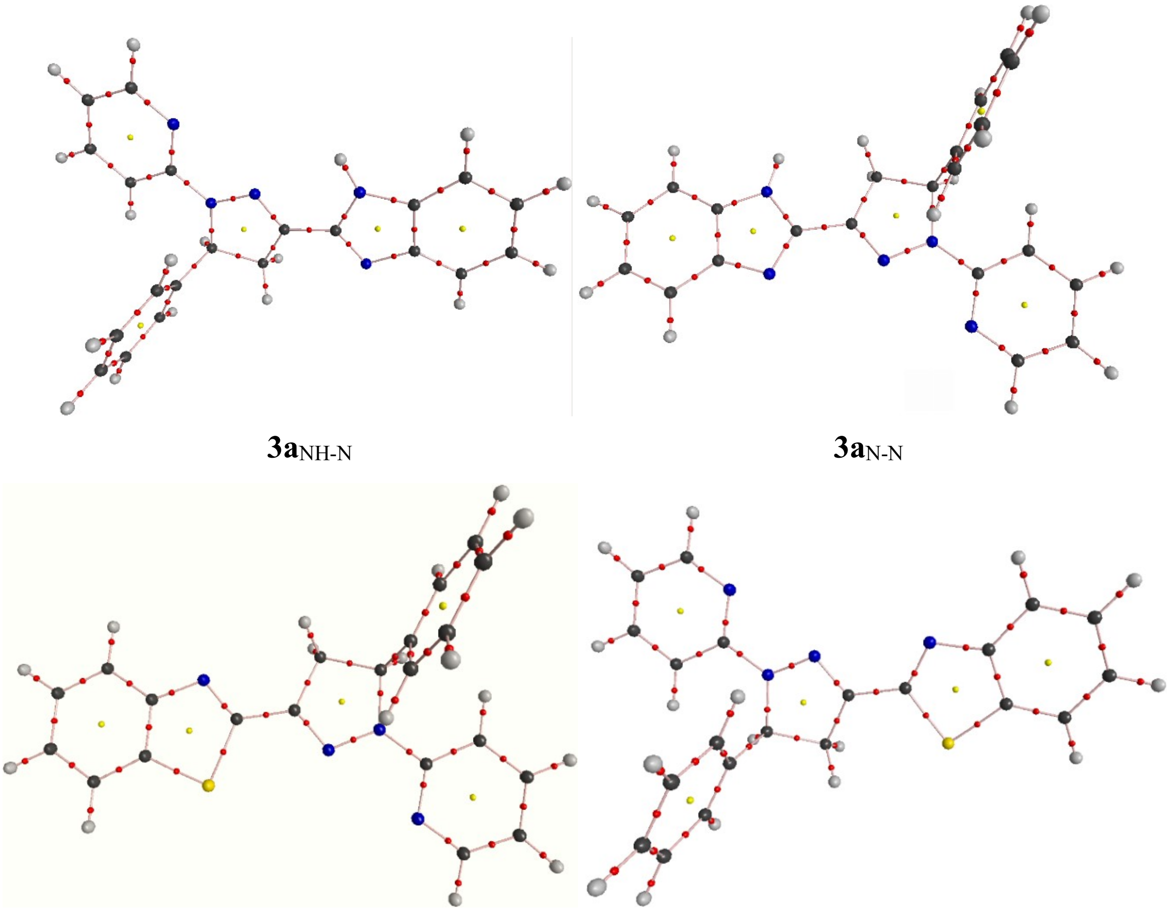

3a$_{NH\text{-}N}$ **3a**$_{N\text{-}N}$

3b$_{S\text{-}N}$ **3b**$_{N\text{-}N}$

Figure 1. Molecular conformations of benzimidazolic derivative **3a** (top) and benzothiazolic derivative **3b** (bottom) according to our quantum-chemical calculations in M06-2x/cc-PVDZ scheme. The bond path, critical points of chemical bonds and cycles (red and yellow points respectively) according to AIM theory are shown as well.

Calculating the complexes geometry of the studied compounds with double-charged cations, we included two Cl^- counter ions in all cases to form a generally electroneutral particle and to model (at least partially) the metal ion coordination sphere. For example, a double-charged cadmium ion coordination number is estimated from 4 to 8 and in a real solution, its free coordination valences will be occupied by acetonitrile molecules. The inclusion of the latter in their explicit form into this calculation would require overly much computational resources.

Depending on spatial proximity of three nitrogen atoms in the corresponding N-N conformations of molecules **3a** and **3b** (or two nitrogen atoms and a sulfur atom in the case of compound **3b**), it can be assumed that these compounds can form a tridentate chelate cavity into which the metal ion enters. This fact was confirmed with our further calculations for the studied compounds complexes with double-charged cations of different size and electronic structure (Mg^{2+}, Zn^{2+}, Cd^{2+}, Hg^{2+}, Pb^{2+}, Ba^{2+}).

Figure 2, as an example, provides the geometry of the complex of compound **3a** with a cadmium ion and two Cl^- counter ions. Complexes with other considered metal ions have a similar structure.

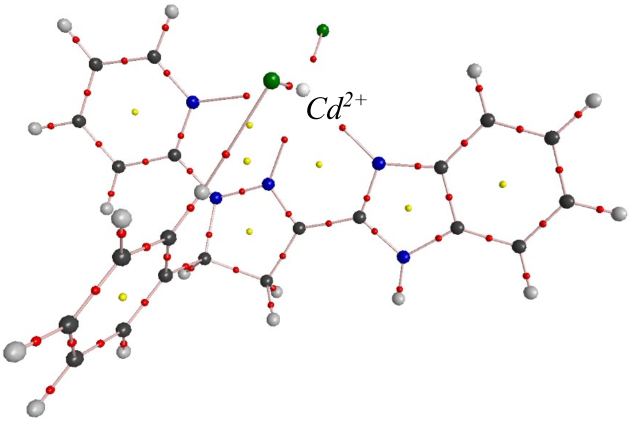

Figure 2. Calculated geometry of compound **3a** complex with cadmium ion and two Cl^- counter ions (M06-2x/cc-PVDZ, ADZP for cadmium atom).

Coordination of Cd^{2+} cation with three nitrogen atoms is confirmed by the existence of corresponding bond paths and (3,-1) type bond critical points. Thus, the assumption we made in our previous publication [33] that there are separate binding sites in 1,3-dihetaryl-5-aryl-pyrazoline molecules such as *"pyrazoline-pyridine"* and *"pyridine-benzazole"* needs definite correction. In addition, one of the chloride anions forms a weak non-classical H-bond with the hydrogen atom in the ortho position of benzene ring-5, which probably makes its contribution to the overall thermodynamic stability of the complex.

To assess the relative stability of the formed complexes, we decided to estimate the pair interaction energies of the cation with the ligand atom forming a corresponding coordination bond with it. With this purpose, we used a semi-empirical model by Espinoza [45], the physical meaning of which is related to the energy characteristics (*virial field function*) of the chemical bond critical point of (3,-1) type. Espinoza's model was initially proposed to estimate approximate energies of hydrogen bonds. Later it was extended to other types of weak noncovalent intermolecular and intramolecular interactions. As an example, we refer to the work [46] with relevant literary references and the authors' discussion on this problem.

The energy of formation of the complex should include the sum of the energies of the individual coordination bonds between the cation and the binding centers in the ligand molecule – three nitrogen atoms or two nitrogen atoms and a sulfur atom. In our opinion, this is the meaningful parameter because it allows approximate estimating the energetic difference in the complexes stability with different cations. The determination of the coordination site nature was carried out by comparing of the sum of energies of individual coordination bonds evaluated according to Espinoza [45]. For example, zinc cation forms stronger coordination bonds with nitrogen atoms of pyrazoline and benzimidazole cycles of compound **3a** in comparison with that of a pyridine cycle. Thus, it can be assumed that the latter contributes relatively less to Zn^{2+} cation binding. Numerical results of the calculations are shown in **Table 1**.

Table 1. Calculated coordination bonds parameters of different metal cations with compounds **3a** and **3b** in their most favorable conformations for the formation of polydentate binding centers

<table>
<tr><th rowspan="2">Cation, ionic radius, Å [47]</th><th colspan="6">Binding center / interaction energy (kcal/mole) / distance
<i>Sums of binding energies with a pair of 2 binding centers out of all three existed</i></th><th rowspan="2">Total interaction energy (kcal/mole)</th></tr>
<tr><th colspan="2">pyridyl (N)</th><th colspan="2">pyrazolinyl (N)</th><th colspan="2">benzimidazolyl (N) / benzothiazolyl (N/S)</th></tr>
<tr><td colspan="8"><i>2-[5-phenyl-1-(pyrid-2-yl)-4,5-dihydro-1H-pyrazol-3-yl]-1H-benzimidazole</i>, 3a</td></tr>
<tr><td rowspan="2">Mg²⁺
0.72 Å</td><td colspan="2">N / 7.65 / 2.312 Å</td><td colspan="2">N / 11.06 / 2.218 Å</td><td colspan="2">N / 8.03 / 2.286 Å</td><td rowspan="2">26.79</td></tr>
<tr><td colspan="3"><i>18.75</i></td><td colspan="3"><i>19.09</i></td></tr>
<tr><td rowspan="2">Zn²⁺
0.74 Å</td><td colspan="2">N / 12.00 / 2.400 Å</td><td colspan="2">N / 20.20 / 2.196 Å</td><td colspan="2">N / 13.34 / 2.346 Å</td><td rowspan="2">45.54</td></tr>
<tr><td colspan="3"><i>32.20</i></td><td colspan="3"><i>33.54</i></td></tr>
<tr><td rowspan="2">Cd²⁺
0.95 Å</td><td colspan="2">N / 5.50 / 2.672 Å</td><td colspan="2">N / 12.56 / 2.397 Å</td><td colspan="2">N / 14.86 / 2.355 Å</td><td rowspan="2">32.92</td></tr>
<tr><td colspan="3"><i>18.06</i></td><td colspan="3"><i>27.42</i></td></tr>
<tr><td rowspan="2">Hg²⁺
1.02 Å</td><td colspan="2">N / 8.91 / 2.723 Å</td><td colspan="2">N / 18.43 / 2.446 Å</td><td colspan="2">N / 15.93 / 2.498 Å</td><td rowspan="2">43.28</td></tr>
<tr><td colspan="3"><i>27.35</i></td><td colspan="3"><i>34.36</i></td></tr>
<tr><td rowspan="2">Pb²⁺
1.19 Å</td><td colspan="2">N / 12.44 / 2.548 Å</td><td colspan="2">N / 16.83 / 2.444 Å</td><td colspan="2">N / 14.10 / 2.499 Å</td><td rowspan="2">43.37</td></tr>
<tr><td colspan="3"><i>29.26</i></td><td colspan="3"><i>30.93</i></td></tr>
<tr><td rowspan="2">Ba²⁺
1.35 Å</td><td colspan="2">N / 6.19 / 2.863 Å</td><td colspan="2">N / 6.45 / 2.809 Å</td><td colspan="2">N / 5.31 / 2.891 Å</td><td rowspan="2">17.95</td></tr>
<tr><td colspan="3"><i>11.62</i></td><td colspan="3"><i>11.76</i></td></tr>
<tr><td colspan="8"><i>2-[5-phenyl-1-(pyrid-2-yl)-4,5-dihydro-1H-pyrazol-3-yl]-benzothiazole,</i> conformation 3b_{N-N}</td></tr>
<tr><td>Mg²⁺</td><td colspan="2">N / 8.18 / 2.319 Å</td><td colspan="2">N / 11.85 / 2.168 Å</td><td colspan="2">N / 6.85 / 2.478 Å</td><td>26.79</td></tr>
</table>

0.72 Å	***19.76***		*18.70*	
Zn^{2+}	N / 14.75 / 2.319 Å	N / 21.96 / 2.168 Å	N / 9.57 / 2.478 Å	46.27
0.74 Å	***36.71***		*31.52*	
Cd^{2+}	N / 8.77 / 2.512 Å	N / 16.45 / 2.329 Å	N / 7.83 / 2.538 Å	33.05
0.95 Å	***25.22***		*24.28*	
Hg^{2+}	N / 11.42 / 2.629 Å	N / 19.53 / 2.427 Å	N / 12.24 / 2.595 Å	43.19
1.02 Å	*30.95*		***32.78***	
Pb^{2+}	N / 13.87 / 2.511 Å	N / 17.71 / 2.429 Å	N / 11.33 / 2.568 Å	42.91
1.19 Å	***31.58***		*29.04*	
Ba^{2+}	N / 5.12 / 2.927 Å	N / 6.99 / 2.801 Å	N / 5.44 / 2.900 Å	17.54
1.35 Å	*12.11*		***12.43***	
2-[5-phenyl-1-(pyrid-2-yl)-4,5-dihydro-1H-pyrazol-3-yl]-benzothiazole, conformation **3b**$_{S\text{-}N}$				
Mg^{2+}	N / 13.82 / 2.122 Å	N / 10.73 / 2.214 Å	S / - / 3.411 Å	24.55
0.72 Å	***24.55***		-	
Zn^{2+}	N / 26.26 / 2.122 Å	N / 19.19 / 2.214 Å	S / 1.03 / 3.411 Å	46.47
0.74 Å	***45.45***		*20.22*	
Cd^{2+}	N / 22.17 / 2.263 Å	N / 14.30 / 2.369 Å	S / 1.26 / 3.452 Å	37.73
0.95 Å	***36.47***		*15.56*	
Hg^{2+}	N / 21.85 / 2.391 Å	N / 16.17 / 2.496 Å	S / 2.10 / 3.347 Å	40.12
1.02 Å	***38.02***		*18.28*	
Pb^{2+}	N / 16.59 / 2.449 Å	N / 3.86 / 2.939 Å	S / 0.76 / 3.934 Å	20.94
1.19 Å	***20.18***		*4.61*	
Ba^{2+}	N / 6.30 / 2.850 Å	N / 4.91 / 2.931 Å	S / 2.60 / 3.307 Å	13.81
1.35 Å	***11.22***		*7.51*	

For each of the cations, **Table 1** shows the sum of the interaction energies with the individual pairs of the heterocycles binding centers: *pyridine* + *pyrazoline* and *pyrazoline* + *benzazole* in order to determine, which of these pairs has a greater affinity to a particular ion, investigated in this article. This kind of analysis was made in order to test our previous hypothesis about the possibility of coordination centers "switching", depending on the nature of the cation coordinated by the ligand.

The paired interactions energy of the cation with the center of its coordination is not the only existing factor that stabilizes the complex. The results presented in **Table 1** do not include the presence of the solvate shell and effective electric field of the solvent. Yet, we have to assume that these numerical data allow to characterize approximately a relative stability of investigated polyheterocyclic ligands complexes with double-charged cations of different ionic radii, most of which belong to the category of toxic heavy metals, environmentally important pollutants.

Molecules **3a** and **3b** contain two electron-excess (azoles) and one electron-deficient (pyridine) ring having nucleophilic centers with unshared electron pairs, which, in fact, are cations coordination sites. In the case of compound **3a**, the cations interact more strongly with nucleophilic centers of the azole rings, and coordination with pyridine nitrogen atom is weaker in all the investigated cases. The dependence of the calculated complexes stability upon ionic radius passes through the plateau for medium-sized ions, and it is also regulated by the hardness/softness of the studied cation. Small (Mg^{2+}) and large (Ba^{2+}) radii ions form weaker complexes, because in the first case, complexation leads to in-plane deformations of the ligand molecule, while in the other case – to out-of-plane ones because a voluminous Ba^{2+} ion does not fit into the potential chelation cavity.

In the case of benzothiazole derivative **3b**, it is possible to coordinate the metal ion not only with nitrogen atoms, as in the case of compound **3a**, but also with benzothiazole sulfur atom. It is well known, that chemical elements such as Pb and Hg have an increased affinity to sulfur. Moreover, this compound conformation with spatially close nitrogen atoms of the pyrazoline cycle and benzothiazole bicycle sulfur atom is more energetically favorable. For the scenario of benzothiazolic nitrogen atom participation in cations binding, molecule **3b** should change its conformation - to unfold the benzothiazole bicycle by 180°. We investigated the possibility of such a conformational rearrangement by calculating the corresponding activation energy of the benzothiazole fragment rotation around the intercyclic ordinary C-C bond. The corresponding transition state was calculated using the method [48]. Thus, the activation energy of the direct conformational rearrangement $\mathbf{3b}_{\text{S-N}} \rightarrow \mathbf{3b}_{\text{N-N}}$ was estimated to be 9.60 kcal/mol, and in the opposite direction - 4.00 kcal/mol. Of course, it is impossible to overcome the energy barrier close to 10 kcal/mole at room temperature, but energy effect of the complexation may be enough to change the spatial arrangement of the chelate center.

Therefore, compound **3b** complexes of two types were included in the calculations: one with the participation of two nitrogen atoms and a sulfur atom (unbound ligand conformation is more plausible), and another with the participation of three nitrogen atoms – a bottom and middle sections of **Table 1**, respectively.

As opposed to compound **3a**, derivative **3b** reveals a more significant effect of pyridine cycle. Probably, a larger volume of the sulfur atom definitely pushes cations closer to the other two binding centers.

The coordination bonds of sulfur atom with the investigated cations were significantly weaker compared to those of the nitrogen atom of thiazole cycle, but, in general, such complexes showed high energetic efficiency.

The greatest affinity to zinc ions was revealed for derivative **3b**. Whereas for the examined series of heavy metals, the binding of cadmium and mercury ions, that are experimentally studied in this work, should be the most efficient.

The calculations let us to conclude that, despite the formation of a general molecular tridentate binding center, cations interaction in compounds **3a,b** shows certain features of complexation sites switching. Thus, with some limitations, the studied molecules can be conditionally classified as "smart ligands", which are able to "programmable adjustment" of their chelated cavity origin depending on the bound metal ion. With cadmium ions, compound **3b** is likely to use a binding center model with a sulfur atom; whereas with mercury ions, the nitrogen atoms of all three heterocyclic ligand subunits "act together" predominantly.

The spectral characteristics of the uncomplexed compounds **3a,b** were studied in polar solvents of close dielectric permittivity - aprotic acetonitrile and proton-donor methanol.

By its chemical nature, the main chromophore fragment of 1,3,5-tri(het)aryl-2-pyrazoline molecules includes "hydrazone" grouping >N-N=C< of the partially hydrogenated pyrazoline cycle, as well as (het)aryl substituents in its positions 1 and 3. This fragment is responsible for the formation of the long-wavelength electronic transition S_0-S_1* in the absorption spectra and the inverse transition S_1*-S_0 in the fluorescence spectra. The substituent in the non-conjugated position 5 of the molecule is seemingly unable to affect luminescent characteristics of the pyrazoline series compounds. However, under certain circumstances it can lead to almost completed fluorescence quenching [49-51]. This phenomenon mechanism has been considered in publications of our and other research groups, but it is still not definitively proven. In the case of benzene ring without electron-accepting substituents in position 5, fluorescence quenching does not occur.

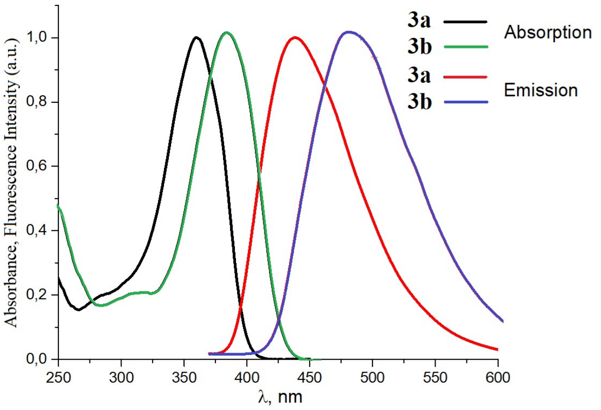

Figure 3. Absorption and fluorescence spectra of compounds **3a** and **3b** in acetonitrile upon excitation at 360 nm.

Thus, with a few exceptions, 1,3,5-triaryl-2-pyrazoline derivatives are considered to be good fluorophores with emission from blue and green to even red spectral range. Typically, the main radiationless photophysical mechanism, that competes with fluorescence emission (and leads to a decrease of the quantum yield of the latter), is the intersystem crossing (ICS) [52]. However, singlet and triplet energy levels of nπ* type, which increase the efficiency of ICS [53, 54], are much higher in pyrazoline derivatives, than the fluorescent state S_1*, and do not play a significant role in the optical properties' formation of this class of compounds. The derivatives studied in this article are typical representatives of the pyrazoline series. The absorption and fluorescence spectra of compounds **3a** and **3b** in acetonitrile are presented in **Figure 3**, the numerical characteristics are shown in **Table 2**.

Table 2. Spectral-luminescent characteristics of pyrazoline derivatives **3a** and **3b** in acetonitrile and methanol

Compound	Solvent	Absorption		Fluorescence			
		λ, nm	ν, cm^{-1}	λ, nm	ν, cm^{-1}	Stokes shift, $\Delta\nu_{ST}$, cm^{-1}	Quantum yield, φ
3a	acetonitrile	361	27700	438	22830	4870	0.80
	methanol	363	27550	446	22420	5130	0.85
3b	acetonitrile	383	26110	479	20880	5230	0.76
	methanol	385	25970	489	20450	5520	0.88

The high fluorescence quantum yields of the studied compounds, which are observed even in polar solvents, are noteworthy. They reveal the absence of significant redistribution of electron density in their molecules during the transition to the electronically excited state and the low probability of highly polar intramolecular charge transfer excited states formation [55, 56], for which fluorescence quenching in a polar environment is typical.

The substitution of benzimidazole moiety in position 3 of the pyrazoline cycle by benzothiazole one leads to a significant long-wavelength shift of the absorption spectra (up to ~ 1500 cm^{-1}/20 nm). This may occur due to a lower electronegativity of the sulfur atom compared to the nitrogen atom of the benzimidazole bicycle.

The change of acetonitrile to methanol solutions causes insignificant changes in the absorption spectra, the observed long-wavelength shift is about only 2 nm. At the same time, fluorescence spectra appeared more responsive to the formation of hydrogen bonds with solvent molecules: fluorescence bands expand slightly and show a bathochromic shift of up to 400 cm^{-1} (up to 10 nm).

In all the studied cases, fluorescence Stokes shifts are within the range of 4900-5500 cm^{-1}. Such values are on the margin between the "normal" and "abnormally high" ranges of this photophysical parameter. This indicates the presence of definite structural relaxation processes in the electronically excited state. They are most likely associated with a certain excited state flattening of the molecular fragment responsible for fluorescence emission, as it takes place in the case of *ortho*-analogs of POPOP [57, 58] previously studied by our research group. So it is obvious that, the conformational changes in the electronically excited state of 1,3,5-traryl-2-pyrazoline derivatives are much smaller than in the above-mentioned class of organic high Stokes shift fluorescent compounds.

Fluorescence quantum yields of the studied derivatives **3a,b** increase up to 6-15% in methanol solution. Probably, the reason for this phenomenon is the increase in the energy of triplet nπ* levels, which is reflected in the decrease of efficiency of radiationless intersystem crossing process [53], that compete with fluorescence emission.

For the studied compounds, spectrophotometric and spectrofluorimetric titration was carried out with salts of selected heavy toxic metals (cadmium nitrate and mercury acetate) in acetonitrile solution, the results of which are shown in **Figure 4** and in **Table 3**.

When adding the cadmium or mercury salts to the acetonitrile solution of the investigated compounds, a long-wavelength absorption bands shift is observed usually. It is also accompanied with a definite decrease of absorption bands intensity. Normally, when titrated with cadmium nitrate, clear isosbestic points are observed, which is an indication of a two-component system (ligand + complex). The fluorescence spectra manifest similar effects.

In the case of cadmium ions, there is no significant fluorescence quenching due to a heavy atom effect, which mechanism is in the increase of ISC rate. Thus, fluorescence of cadmium complexes is observed in the spectra of compounds **3a,b** as an appearing shoulder on the long-wavelength wing of the ligand emission band. In this case, the principle of ratiometric fluorescence detection can be applied [59-61]. Its fundamental advantage over traditional intensometric techniques is an absolute fluorescent signal formation in the form of emission intensities ratio at different wavelengths for the same sample. Ratiometric analytical signal does not depend on the excitation light intensity and does not require the application of special standards, which are traditionally used, for example, in the calculation of luminescence quantum yields [34]. The complexation equilibrium constants, calculated from the absorption and fluorescence spectra, were quite close in their value. This fact allowed us to conclude that the ligand-cation interaction occurs within a purely static mechanism when complexes are formed exclusively in the ground state.

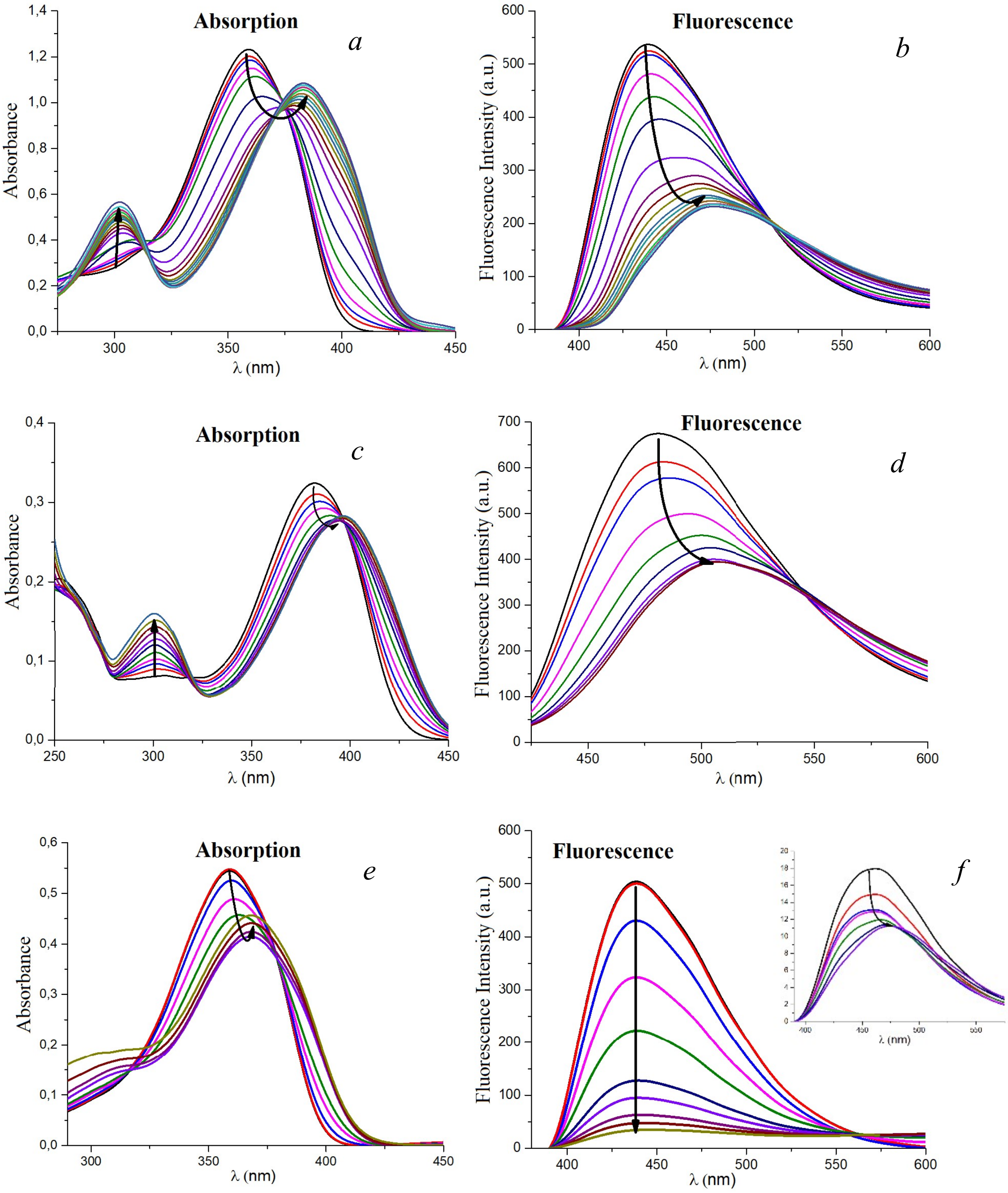

Figure 4. Absorption and fluorescence spectra of compounds **3a,b** upon addition of Cd^{2+} and Hg^{2+} salts to their acetonitrile solution.

a: spectrophotometric titration of **3a** with cadmium nitrate, *b*: fluorimetric titration of **3a** with cadmium nitrate, *c*: spectrophotometric titration of **3b** with cadmium nitrate, *d*: fluorimetric titration of **3b** with cadmium nitrate, *e*: spectrophotometric titration of **3a** with mercury acetate, *f*: fluorimetric titration of **3a** with mercury acetate, the inset shows fluorescence spectra changes at high concentrations of added mercury salt.

Interaction with Hg^{2+} ions in the studied compounds absorption spectra shows effects similar to the observed ones in the case of cadmium ions, except the bands shift in the spectrum during complexation was less distinct. In the emission spectra, on the contrary, the main feature was the effective and almost complete fluorescence quenching. Mercury cation is, in general, a recognized fluorescence quencher relying on the mechanisms of heavy atom and electron transfer [62]. Thus, the number of sensory compounds that interact with the discussed cation directly, and demonstrate an increase in fluorescence intensity during complexation, is quite limited [63]. Compounds **3a,b** fluorescence is quite expectedly quenched at interaction with mercury ions. Only in the case of **3a** at the end of the titration, the long-wavelength shift of the almost extinct band of the complex becomes recognizable (**Figure 3*f***).

Also we qualitatively tested the relative stability of the formed cadmium and mercury complexes of compounds **3a,b** by adding one of the strongest complexing agents – Trilon B (Tetrasodium EDTA) to the mixture obtained at the end of the titration. It was found out that Trilon B destroyed complexes with mercury ions, as it was testified by the appearance of intense fluorescence of unbound ligand. At the same time, Trilon B did not have a similar effect on cadmium complexes because the optical characteristics of the solution did not show any changes.

Table 3. Complexation constants of compounds **3a,b** with cadmium and mercury ions in acetonitrile obtained by spectrophotometric titration

Compound	**3a**		**3b**	
logK	Cd^{2+}	Hg^{2+}	Cd^{2+}	Hg^{2+}
	4.67	5.41	3.54	4.39

The experimentally determined sensitivity of compound **3a** to Cd^{2+} ions, which reflects its logK=4.67, is comparable with that of many other probes synthesized and reported during the last decade: 3.34 [64], 3.63 [65], 4.12 [66], 5.72 [67], 5.81 [32]. Thiazolic derivative **3b** is less sensitive to cadmium (see **Table 3**). The same tendency is typical to **3a** and **3b** complexing with Hg^{2+}. However, in spite of the fact that several authors report lower binding constants for their “newly synthesized effective sensing molecules”, for example, 3.23 [68], 3.58 [69], 4.19 [66], 5.27 [70], one can find examples of much more efficient chemosensors with their logK 5.67 [71], 6.53 [32], 7.06 [72], 7.93 [73] and even 9.60 [74].

Thus, the studied polyheterocyclic 1,3,5-triaryl-2-pyrazoline derivatives **3a,b** show moderate sensitivity to cadmium and mercury cations in acetonitrile at a level of 10^{-6}-10^{-7} M, which allows spectrophotometric and/or spectrofluorimetric analysis of these toxic metals in natural samples only when the maximum allowable concentrations are exceeded.

Conclusions

Polyheterocyclic derivatives of 1,3,5-triaryl-2-pyrazoline with pyridine ring in position 1 and benzimidazole or benzothiazole bicycles in position 3 of the central pyrazoline nucleus have been synthesized, the spectral-fluorescent properties and complexation with cadmium and mercury ions, which belong to the group of heavy metals – dangerous environmental pollutants, have been investigated. Computer simulations of the studied derivatives complexing with double-charged metal ions, Mg^{2+}, Zn^{2+}, Cd^{2+}, Hg^{2+}, Pb^{2+} and Ba^{2+}, have been carried out. Our calculations show that the three heteroatoms of the studied compounds, that belong to the three different heterocycles, form a tridentate chelate cavity, which, depending on the bound cation, in a certain sense, adapting to its nature. It affects the energy of the formed coordination bonds: in the case of the benzimidazole derivative, interaction of metal ion with pyrazoline and benzimidazole cycles nitrogen atoms becomes more important, whereas in the benzothiazole derivative, interaction of complex central ion with pyrazoline and pyridine cycles nitrogen atoms plays a key role. In the latter case, the adjustment of the chelation cavity to the nature of the cation was revealed, which allowed classifying this compound as "smart ligand".

Spectral characteristics of the studied compounds demonstrated sensitivity to the medium proton-donor ability. This was recognized as a perceptible long-wavelength shift of emission bands, which was accompanied with a small increase in the fluorescence quantum yield. Complexation with metal ions in acetonitrile leads to long-wavelength shifts of absorption and fluorescence bands, as well as a noticeable intensity decrease of the latter, especially in the case of Hg^{2+} ions. There has been established the fact of mercury complexes destruction at Trilon B (Tetrasodium EDTA) addition to the solution, as well as the absence of influence of this effective complexing agent on the complexes of investigated compounds with cadmium ions.

Acknowledgements

This work was supported in part by a research grant of the Ministry of Education and Science of Ukraine 0119U002536. The investigation was carried out using the computing facilities of the joint computer cluster of SSI “Institute for Single Crystals” and Institute for Scintillation Materials of the National Academy of Science of Ukraine incorporated into Ukrainian National Grid.

References

[1] Nolan EM, Lippard SJ. Small-Molecule Fluorescent Sensors for Investigating Zinc Metalloneurochemistry. Accounts of Chemical Research. 2009;42(1):193-203.

[2] Wu J, Liu W, Ge J, Zhang H, Wang P. New sensing mechanisms for design of fluorescent chemosensors emerging in recent years. Chemical Society Reviews. 2011;40(7):3483-95.

[3] Li M, Gou H, Al-Ogaidi I, Wu N. Nanostructured Sensors for Detection of Heavy Metals: A Review. ACS Sustainable Chemistry & Engineering. 2013;1(7):713-23.

[4] Carter KP, Young AM, Palmer AE. Fluorescent Sensors for Measuring Metal Ions in Living Systems. Chemical Reviews. 2014;114(8):4564-601.

[5] Chowdhury S, Rooj B, Dutta A, Mandal U. Review on Recent Advances in Metal Ions Sensing Using

Different Fluorescent Probes. Journal of Fluorescence. 2018;28(4):999-1021.

[6] Patil NS, Dhake RB, Ahamed MI, Fegade U. A Mini Review on Organic Chemosensors for Cation Recognition (2013-19). Journal of Fluorescence. 2020;30(6):1295-330.

[7] Shao N, Gao X, Wang H, Yang R, Chan W. Spiropyran-based optical approaches for mercury ion sensing: Improving sensitivity and selectivity via cooperative ligation interactions using cysteine. Analytica Chimica Acta. 2009;655(1-2):1-7.

[8] Baldrighi M, Locatelli G, Desper J, Aakeröy CB, Giordani S. Probing Metal Ion Complexation of Ligands with Multiple Metal Binding Sites: The Case of Spiropyrans. Chemistry – A European Journal. 2016;22(39):13976-84.

[9] Eshtiagh-Hosseini H, Aghabozorg H, Mirzaei M, Amini MM, Chen Y-G, Shokrollahi A, et al. Diversity in coordination behavior of dipicolinic acid with lead(II), calcium(II), and nickel(II) in the presence of pyrazine and 2-amino-4-methylpyridine spacers in construction of three supramolecular architectures. Journal of Molecular Structure. 2010;973(1-3):180-9.

[10] Koner RR, Sinha S, Kumar S, Nandi CK, Ghosh S. 2-Aminopyridine derivative as fluorescence 'On–Off' molecular switch for selective detection of Fe3+/Hg2+. Tetrahedron Letters. 2012;53(18):2302-7.

[11] Mandal S, Ghosh S, Banerjee C, Kuchlyan J, Sarkar N. Unique Photophysical Behavior of 2,2′-Bipyridine-3,3′-diol in DMSO–Water Binary Mixtures: Potential Application for Fluorescence Sensing of Zn^{2+} Based on the Inhibition of Excited-State Intramolecular Double Proton Transfer. J Phys Chem B. 2013;117(40):12212-23.

[12] Vosough Razavi B, Badiei A, Lashgari N, Mohammadi Ziarani G. 2,6-Bis(2-Benzimidazolyl)Pyridine Fluorescent Red-Shifted Sensor for Recognition of Zinc(II) and a Calorimetric Sensor for Iron Ions. Journal of Fluorescence. 2016;26(5):1723-8.

[13] Ruan Y-B, Xie J. Unexpected highly selective fluorescence 'turn-on' and ratiometric detection of Hg2+ based on fluorescein platform. Tetrahedron. 2011;67(45):8717-23.

[14] Yang X-F, Li Y, Bai Q. A highly selective and sensitive fluorescein-based chemodosimeter for Hg2+ ions in aqueous media. Analytica Chimica Acta. 2007;584(1):95-100.

[15] Chen J, Zheng A, Chen A, Gao Y, He C, Kai X, et al. A functionalized gold nanoparticles and Rhodamine 6G based fluorescent sensor for high sensitive and selective detection of mercury(II) in environmental water samples. Analytica Chimica Acta. 2007;599(1):134-42.

[16] Huang J, Xu Y, Qian X. A Rhodamine-Based Hg^{2+} Sensor with High Selectivity and Sensitivity in Aqueous Solution: A NS2-Containing Receptor. The Journal of Organic Chemistry. 2009;74(5):2167-70.

[17] Mao J, He Q, Liu W. An rhodamine-based fluorescence probe for iron(III) ion determination in aqueous solution. Talanta. 2010;80(5):2093-8.

[18] Kumar M, Kumar N, Bhalla V. Rhodamine appended thiacalix[4]arene of 1,3-alternate conformation for nanomolar detection of Hg2+ ions. Sensors and Actuators B: Chemical. 2012;161(1):311-6.

[19] Ling L, Zhao Y, Du J, Xiao D. An optical sensor for mercuric ion based on immobilization of Rhodamine B derivative in PVC membrane. Talanta. 2012;91:65-71.

[20] Wang F, Nam S-W, Guo Z, Park S, Yoon J. A new rhodamine derivative bearing benzothiazole and thiocarbonyl moieties as a highly selective fluorescent and colorimetric chemodosimeter for Hg2+. Sensors and Actuators B: Chemical. 2012;161(1):948-53.

[21] Kuchlyan J, Basak S, Dutta D, Das AK, Mal D, Sarkar N. A new rhodamine derived fluorescent sensor: Detection of Hg2+ at cellular level. Chemical Physics Letters. 2017;673:84-8.

[22] Wan J, Zhang K, Li C, Li Y, Niu S. A novel fluorescent chemosensor based on a rhodamine 6G derivative for the detection of Pb^{2+} ion. Sens Act B: Chem. 2017;246:696-702.

[23] Carturan S, Quaranta A, Maggioni G, Bonafini M, Della Mea G. 3-Hydroxyflavone-based wavelength shifting systems for near UV optical sensors. Sensors and Actuators A: Physical. 2004;113(3):288-92.

[24] de la Rosa-Romo LM, Oropeza-Guzmán MT, Olivas-Sarabia A, Pina-Luis G. Flavone functionalized magnetic nanoparticles: A new fluorescent sensor for Cu^{2+} ions with nanomolar detection limit. Sensors and Actuators B: Chemical. 2016;233:459-68.

[25] Gao H, Wu X. A 3-hydroxyflavone derivative as fluorescence chemosensor for copper and zinc ions. Chemistry of Heterocyclic Compounds. 2018;54(2):125-129.

[26] Yang S, Hu Z, Guo D. Novel flavonoid derivatives and their corresponding rare earth complexes: Synthesis and luminescent properties. Journal of Luminescence. 2021;237:118195.

[27] Michalík M, Biela M, Cagardová D, Lukeš V. Chelates of 3- and 5-hydroxyflavone: Quantum chemical study. Chemical Physics Letters. 2021;762:138142.

[28] Kamecki F, Marcucci C, Ferreira-Gomes M, Sabatier L, Knez D, Gobec S, et al. 2'-Hydroxy-4',5'-dimethyl-4-dimethylaminochalcone, a novel fluorescent flavonoid with capacity to detect aluminium in cells and modulate Alzheimer's disease targets. J Photochem Photobiol A: Chem. 2021;409:113137.

[29] Qin T, Liu B, Xu Z, Yao G, Xu H, Zhao C. Flavonol-based small-molecule fluorescent probes. Sens Act B: Chem. 2021;336:129718.

[30] Drabovich AP, Berezovski MV, Musheev MU, Krylov SN. Selection of Smart Small-Molecule Ligands: The Proof of Principle. Analytical Chemistry. 2008;81(1):490-4.

[31] Dondaine L, Escudero D, Ali M, Richard P, Denat F, Bettaieb A, et al. Coumarin-Phosphine-Based Smart Probes for Tracking Biologically Relevant Metal Complexes: From Theoretical to Biological Investigations. European Journal of Inorganic Chemistry. 2016;2016(4):545-53.

[32] Banerjee M, Ghosh M, Ta S, Das J, Das D. A smart optical probe for detection and discrimination of Zn2+, Cd2+ and Hg2+ at nano-molar level in real samples. Journal of Photochemistry and Photobiology A: Chemistry. 2019;377:286-97.

[33] Chumak AY, Kordubailo MV, Vodolazhenko MA, Kotliar VM, Doroshenko AO. Derivatives of 1,3,5 triaryl-2-pyrazoline with additional heterocyclic moieties in position 1 as potential fluorescent chemosensing compounds for detection of polyvalent metals cations. Kharkiv University Bulletin Chemical Series. 2018;31(54):32-43.

[34] Melhuish WH. Absolute spectrofluorometry. Journal of Research of the National Institute of Standards and Technology Sec A: Physical Chemistry. 1972;76A(6):547-60.

[35] Frisch MJ, Trucks GW, Schlegel HB, Scuseria GE, Robb MA, Cheeseman JR, et al. Gaussian 09, Revision B.01. Wallingford CT: Gaussian, Inc.; 2010.

[36] Zhao Y, Schultz NE, Truhlar DG. Design of Density Functionals by Combining the Method of Constraint Satisfaction with Parametrization for Thermochemistry, Thermochemical Kinetics, and Noncovalent Interactions. Journal of Chemical Theory and Computation. 2006;2(2):364-82.

[37] Woon DE, Dunning TH. Gaussian basis sets for use in correlated molecular calculations. III. The atoms aluminum through argon. The Journal of Chemical Physics. 1993;98(2):1358-71.

[38] Canal Neto A, Muniz EP, Centoducatte R, Jorge FE. Gaussian basis sets for correlated wave functions. Hydrogen, helium, first- and second-row atoms. Journal

of Molecular Structure: THEOCHEM. 2005;718(1):219-24.

[39] de Oliveira PJP, Barros CL, Jorge FE, Canal Neto A, Campos M. Augmented Gaussian basis set of double zeta valence quality for the atoms Rb and Y–Xe: Application in DFT calculations of molecular electric properties. Journal of Molecular Structure: THEOCHEM. 2010;948(1):43-6.

[40] Bader RFW. Atoms in molecules. Accounts of Chemical Research. 1985;18(1):15-8.

[41] Bader RFW. A quantum theory of molecular structure and its applications. Chemical Reviews. 1991;91(5):893-928.

[42] Bader RFW. A Bond Path: A Universal Indicator of Bonded Interactions. The Journal of Physical Chemistry A. 1998;102(37):7314-23.

[43] Biegler-König F, Schönbohm J, Bayles D. AIM2000 - A Program to Analyze and Visualize Atoms in Molecules. Journal of Computational Chemistry. 2001;22(5):545-59.

[44] Dunning TH, Hay PJ. Gaussian Basis Sets for Molecular Calculations. In: Schaefer HF, editor. Methods of Electronic Structure Theory. Boston, MA: Springer US; 1977. p. 1-27.

[45] Espinosa E, Molins E, Lecomte C. Hydrogen bond strengths revealed by topological analyses of experimentally observed electron densities. Chemical Physics Letters. 1998;285(3):170-3.

[46] Zhikol OA, Shishkin OV. Estimating stacking interaction energy using atom in molecules properties: Homodimers of benzene and pyridine. International Journal of Quantum Chemistry. 2012;112(18):3008-17.

[47] Shannon R. Revised effective ionic radii and systematic studies of interatomic distances in halides and chalcogenides. Acta Crystallogr, Sect A: Found Adv. 1976;32(5):751-67.

[48] Peng C, Ayala PY, Schlegel HB, Frisch MJ. Using redundant internal coordinates to optimize equilibrium geometries and transition states. J Comput Chem. 1996;17(1):49-56.

[49] Doroshenko AO, Skripkina VT, Schershukov VM, Ponomaryov OA. Fluorescence Quenching in Bichromophoric Systems with Nonconjugated Chromophores: 5-Substituted Derivatives of 1,3,5-Triaryl-2-Pyrazoline. Journal of Fluorescence. 1997;7:131-8.

[50] Krasovitskii BM, Pereyaslova DG, Skripkina VT, Yagupolskii LM, Popov VI. Organic luminophores with fluorine-containing substituents. Dyes and Pigments. 1988;9(1):21-35.

[51] Letrun R, Lang B, Yushchenko O, Wilcken R, Svechkarev D, Kolodieznyi D, et al. Excited-state dynamics of a molecular dyad with two orthogonally-oriented fluorophores. Physical Chemistry Chemical Physics. 2018;20(48):30219-30.

[52] Ermolaev VL, Sveshnikova EB. Limits to the applicability of the rule of equality to unity of the sum of quantum yields of fluorescence and transition to the triplet state for complex organic molecules in the condensed phase (A review). Optics and Spectroscopy. 2015;119(4):642-55.

[53] Plotnikov VG. Regularities of the Processes of Radiationless Conversion in Polyatomic Molecules. International Journal of Quantum Chemistry. 1979;16:527-41.

[54] Plotnikov VG. Theoretical Foundations of the Classification of Molecules by Luminescence Spectra. Russian Chemical Reviews. 1980;49(2):327-61.

[55] Lippert E, Rettig W, Bonacic-Koutecky V, Heisel F, Miehe JA. Photophysics of internal twisting. In: Prigogine I, Rice SA, editors. Advances in Chemical physics. 68. Hoboken, NJ, USA: John Wiley & Sons, Inc.; 1987. p. 1-174.

[56] Grabowski ZR, Rotkiewicz K, Rettig W. Structural Changes Accompanying Intramolecular Electron Transfer: Focus on Twisted Intramolecular Charge-Transfer States and Structures. Chemical Reviews. 2003;103(10):3899-4032.

[57] Doroshenko AO, Kirichenko AV, Mitina VG, Ponomaryov OA. Spectral properties and dynamics of the excited state structural relaxation of the ortho analogues of POPOP — Effective abnormally large Stokes shift luminophores. Journal of Photochemistry and Photobiology A: Chemistry. 1996;94(1):15-26.

[58] Iliashenko R, Zozulia O, Doroshenko A. High Stokes shift long-wavelength energy gap regulated fluorescence in the series of nitro/dimethylamino-substituted ortho-analogs of POPOP. Open Chemistry. 2011;9(6):962-71.

[59] Demchenko AP. The problem of self-calibration of fluorescence signal in microscale sensor systems. Lab on a Chip. 2005;5(11):1210.

[60] Demchenko AP. The Concept of λ-Ratiometry in Fluorescence Sensing and Imaging. Journal of Fluorescence. 2010;20(5):1099-128.

[61] Demchenko AP. Practical aspects of wavelength ratiometry in the studies of intermolecular interactions. Journal of Molecular Structure. 2014;1077:51-67.

[62] Nolan EM, Lippard SJ. Tools and Tactics for the Optical Detection of Mercuric Ion. Chemical Reviews. 2008;108(9):3443-80.

[63] Callan JF, de Silva AP, Magri DC. Luminescent sensors and switches in the early 21st century. Tetrahedron. 2005;61(36):8551-88.

[64] Ellairaja S, Manikandan R, Vijayan MT, Rajagopal S, Vasantha VS. A simple highly sensitive and selective TURN-ON fluorescent chemosensor for the detection of cadmium ions in physiological conditions. RSC Advances. 2015;5(78):63287-95.

[65] Ma J, Dong Y, Yu Z, Wu Y, Zhao Z. A pyridine based Schiff base as a selective and sensitive fluorescent probe for cadmium ions with “turn-on” fluorescence responses. New Journal of Chemistry. 2022;46(7):3348-57.

[66] Li M, Lu H-Y, Liu R-L, Chen J-D, Chen C-F. Turn-On Fluorescent Sensor for Selective Detection of Zn2+, Cd2+, and Hg2+ in Water. J Org Chem. 2012;77(7):3670-3.

[67] Sharma P, Bhogal S, Lealam A, Kumar S, Yusuf M, Malik AK. Experimental and Theoretical Studies of the Pyrazoline Derivative 5-(4-methylphenyl)-3-(5-methylfuran-2-yl)-1-phenyl-4,5-dihydro-1H-Pyrazole and its Application for Selective Detection of Cd2+ ion as Fluorescent Sensor. J Fluor. 2022;32(3):969-81.

[68] Wang H-F, Wu S-P. Highly selective fluorescent sensors for mercury(II) ions and their applications in living cell imaging. Tetrahedron. 2013;69(8):1965-9.

[69] Kao S-L, Wu S-P. A fluorescent turn-on probe for Hg(II) based on an NTe_2 chelating motif and its application in living cell imaging. Sens Act B: Chem. 2015;212:382-8.

[70] Vedamalai M, Wu S-P. A BODIPY-based colorimetric and fluorometric chemosensor for Hg(ii) ions and its application to living cell imaging. Organic & Biomolecular Chemistry. 2012;10(28):5410-6.

[71] Bozkurt E, Gul HI. Selective fluorometric “Turn-off” sensing for Hg2+ with pyrazoline compound and its application in real water sample analysis. Inorganica Chimica Acta. 2020;502:119288.

[72] Saleem M, Khang CH, kim M-H, Lee KH. Chromo/Fluorogenic Detection of Co2+, Hg2+ and Cu2+ by the Simple Schiff Base Sensor. J Fluor. 2015;26(1):11-22.

[73] Svechkarev D, Dereka B, Doroshenko A. Mercury Ions Complexation with a Series of Heterocyclic Derivatives of 3-Hydroxychromone: Spectral Effects and Prospects for Ultrasensitive Hg^{2+} Probing. The Journal of Physical Chemistry A. 2011;115(17):4223-30.

[74] Gauthama BU, Narayana B, Sarojini BK, Suresh NK, Sangappa Y, Kudva AK, et al. Colorimetric “off–on” fluorescent probe for selective detection of toxic Hg2+ based on rhodamine and its application for in-vivo bioimaging. Microchemical Journal. 2021;166:106233.